Osteoporos Int (2012) 23:305–315
DOI 10.1007/s00198-011-1758-z

ORIGINAL ARTICLE

Effects of strontium ranelate and alendronate on bone microstructure in women with osteoporosis

Results of a 2-year study

R. Rizzoli · R. D. Chapurlat · J.-M. Laroche · M. A. Krieg · T. Thomas · I. Frieling · S. Boutroy · A. Laib · O. Bock · D. Felsenberg

Received: 13 May 2011 / Accepted: 11 July 2011 / Published online: 10 September 2011

Abstract
Summary Strontium ranelate appears to influence more than alendronate distal tibia bone microstructure as assessed by high-resolution peripheral quantitative computed tomography (HR-pQCT), and biomechanically relevant parameters as assessed by micro-finite element analysis (μFEA), over 2 years, in postmenopausal osteoporotic women.
Introduction Bone microstructure changes are a target in osteoporosis treatment to increase bone strength and reduce fracture risk.
Methods Using HR-pQCT, we investigated the effects on distal tibia and radius microstructure of strontium ranelate (SrRan; 2 g/day) or alendronate (70 mg/week) for 2 years in postmenopausal osteoporotic women. This exploratory randomized, double-blind trial evaluated HR-pQCT and FEA parameters, areal bone mineral density (BMD), and bone turnover markers.
Results In the intention-to-treat population (n=83, age: 64±8 years; lumbar T-score: −2.8±0.8 [DXA]), distal tibia Cortical Thickness (CTh) and Density (DCort), and cancellous BV/TV increased by 6.3%, 1.4%, and 2.5%, respectively (all P<0.005), with SrRan, but not with alendronate (0.9%, 0.4%, and 0.8%, NS) (P<0.05 for all above between-group differences). Difference for CTh evaluated with a distance transformation method was close to significance (P=0.06). The estimated failure load increased with SrRan (+2.1%, P<0.005), not with alendronate (−0.6%, NS) (between-group difference, P<0.01). Cortical stress was lower with SrRan (P<0.05); both treatments decreased trabecular stress. At distal radius, there was no between-group difference other than DCort (P<0.05). Bone turnover markers decreased with alendronate; bALP increased (+21%) and serum-CTX-I decreased (−1%) after 2 years of SrRan (between-group difference at each time point for both markers, P<0.0001). Both treatments were well tolerated.
Conclusions Within the constraints of HR-pQCT method, and while a possible artefactual contribution of strontium

R. Rizzoli (✉)
Division of Bone Diseases, Department of Medical Specialties,
Geneva University Hospitals and Faculty of Medicine,
1211 Geneva 14, Switzerland
e-mail: Rene.Rizzoli@unige.ch

R. D. Chapurlat · S. Boutroy
INSERM U831, Université de Lyon, Edouard Herriot Hospital,
Lyon, France

J.-M. Laroche
Rangueil Hospital,
Toulouse, France

M. A. Krieg
Department of Musculoskeletal Medicine, CHUV,
Lausanne, Switzerland

T. Thomas
INSERM U890, University Hospital,
Saint-Etienne, France

I. Frieling
Osteoporosezentrum,
Hamburg, Germany

A. Laib
SCANCO Medical AG,
Bruettisellen, Switzerland

O. Bock · D. Felsenberg
Charité – Universitätsmedizin Berlin, Campus Benjamin Franklin,
Centre of Muscle and Bone Research, Free University and
Humboldt University,
Berlin, Germany

cannot be quantified, SrRan appeared to influence distal tibia bone microstructure and FEA-determined biomechanical parameters more than alendronate. However, the magnitude of the differences is unclear and requires confirmation with another method.

Keywords Alendronate · Finite elements analysis · HR-pQCT · Microstructure · Osteoporosis · Strontium ranelate

Introduction

Fragility fractures result from a low bone resistance to an external force [1, 2]. Bone strength is determined by material and structural properties [1, 2]. There is a variety of new techniques available in bone imaging for the determination of bone microstructure [3, 4], providing an increasing amount of evidence for the links between bone strength and structure in osteoporosis. High-resolution peripheral quantitative computed tomography (HR-pQCT) gives three-dimensional datasets providing estimate of bone geometry, cortical and trabecular structures [5, 6]. This technique has confirmed that an impairment in trabecular and/or cortical structures is associated with increased risk for vertebral and non-vertebral fracture in postmenopausal women in case-control studies [7–11] HR-pQCT also allows for a non-invasive quantification of bone strength and mechanical features of cortical and trabecular bone by using finite element analysis (FEA) [12] Failure load predicted by a linear FE model is consistent with experimental testing [13]. Moreover, radius [14, 15] and radius and tibia [16] bone mechanical properties as assessed by FEA are associated with fragility fracture independently of bone mineral density (DMD) or microstructure in postmenopausal women. HR-pQCT images can be used either as continuous models with a gray-scale voxel conversion to modulus of elasticity, similarly to clinical CT data, or as binary images using fixed homogeneous material properties. The first model implicitly takes into account partial volume effects and changes in tissue mineralization, which may result from the osteoporosis treatment, whereas the second model considers changes in bone microstructure independently of material effects. Both models provide good estimate of distal radius apparent strength, even though the correlation is slightly higher with scaled tissue modulus than homogeneous modulus models (R^2=0.983 versus R^2=0.972, P<0.05, n=31) [14].

The improvement of trabecular and cortical structure is a therapeutic target in osteoporosis since this may increase bone strength and reduce fracture risk. The study described herein was designed to explore the effects of a 2-year treatment with strontium ranelate, as compared to alendronate, on bone microstructure in postmenopausal women with osteoporosis. Strontium ranelate reduces the risk of vertebral and non-vertebral fractures in postmenopausal women with osteoporosis [15, 16]. Histomorphometric and micro-CT analyses of bone biopsies of strontium ranelate-treated women have suggested improvements in trabecular and cortical microstructure [17]. The bone resorption inhibitor alendronate has anti-fracture efficacy [18]. While histomorphometric analyses with alendronate indicate maintenance of trabecular and cortical structure, they failed to detect any improvement [19]. Our study involved HR-pQCT analyses in treated women on both distal tibia and distal radius, including FEA at the tibia as well as evaluation of areal BMD of the spine and the hip by DXA, and of bone turnover markers (bone alkaline phosphatase [b-ALP] for bone formation, and serum C-telopeptide cross-links of type-1 collagen [S-CTX-I] for bone resorption). The preplanned interim 1-year analysis of the here discussed study has been previously published [20], and this report presents now the final analysis of the whole study.

Methods

Study design

The study design has extensively been described previously [20]. Briefly, this randomized, double-blind, double-dummy, 2-year-long trial was carried out in eight centers across four countries (Australia, France, Germany, and Switzerland). Ambulatory Caucasian postmenopausal women, aged 50 years and over, were included if they had a lumbar (L1-L4), femoral neck, or total hip T-score of less than −2.5, as assessed by DXA. Exclusion criteria were body mass index (BMI) >30 or <18 kg/m^2, as well as diseases and treatments that interfere with bone metabolism (including bisphosphonate for more than 1 year or strontium ranelate, in the immediately preceding year). The protocol was approved by local ethics committees and complied with the ethical principles of the Declaration of Helsinki, 1964, revised in Tokyo 2004. All participants gave their written informed consent prior to their participation. The trial was registered with www.controlled-trials.com as ISRCTN82719233.

Participants were randomly assigned to either strontium ranelate (2 g/day; 1 sachet/day at bedtime, plus 1 capsule placebo/week in the morning) or alendronate 70 mg/week (1 capsule/week in the morning, plus 1 sachet placebo/day at bedtime). The treatments and placebo were similar in terms of appearance, and sachet or capsule weight. All patients received additional calcium (500 mg) and vitamin D (400 IU) supplements (1 tablet/day at lunchtime).

The primary endpoints of this exploratory study were HR-pQCT parameters (all parameters measured at cortical and trabecular level, described below). Secondary criteria were FEA parameters, lumbar and femoral neck aBMD, markers of bone resorption and formation as well as safety.

HR-pQCT analysis

HR-pQCT (XtremCT, Scanco Medical AG, Bruttisellen, Switzerland) examinations were performed on the non-dominant distal tibia and distal radius at baseline, 3 and 6 months, and then every 6 months up to 2 years, as previously described [20]. The region of interest consisted of 110 slices measured proximally to a 22.5-mm point from the distal joint limit for the tibia, and a 9.5-mm point from the most proximal location of the subchondral plate for the radius. Scans were analyzed in a central facility (Scanco Medical) by assessors blinded to the treatment assignment. A scan was considered as assessable if it was rated as being of a very good or good quality (i.e., without movement artifacts, or minor movements that did not affect the integrity of the cortical circumference). This was the case for 96% of examinations at the distal tibia and 77% at the distal radius. Quality control was centrally reviewed on a daily basis, and devices were cross-calibrated with a density phantom and an anthropomorphic phantom.

HR-pQCT data were processed as described [5, 20–22]. The parameters reported were cortical bone density (D_{Cort}, cortical volumetric BMD), cross-sectional area (CSA), cortical thickness (CTh, mean cortical volume divided by the outer bone perimeter), cortical porosity, trabecular bone density (D_{trab}, trabecular volumetric BMD), bone volume fraction (BV/TV, trabecular bone volume to tissue volume, calculated using trabecular density/1200 mgHA/cm^3), and trabecular number (TbN), thickness (TbTh), and separation (TbSp). In a second series of analysis, CTh, TbTh, and TbSp were also measured using another software, whereby the parameters were not derived from density, but directly assessed using a distance transformation approach [5]. Moreover, cortical porosity was evaluated after a dual segmentation process of the cortex, as described by Burghardt et al. [23], and Nishiyama et al. [24]. These analyses were a post-hoc analysis.

Finite element analysis

Finite element meshes of the tibia were generated directly from binary or gray-level HR-pQCT images by the voxel conversion approach [25], using Image Processing Language (IPL) software (Scanco Medical). Linear FEA was applied to simulate a uniaxial compression test in the axial direction using the FE-solver included in the IPL software v1.12. Material properties chosen were isotropic and elastic for both models, with a Poisson's ratio of 0.3. For the segmented model, cortical and trabecular bone elements were distinguished using the standard HR-pQCT protocol and assigned different elastic properties: Young's modulus was 20 and 17 GPa for cortical and trabecular bone, respectively. For the continuum model, trabecular and cortical bone were treated in the same way and the gray-level images were binned to 8-bit data, thus allowing 127 different moduli, calculated, based on the relation developed by Homminga et al. [26] and MacNeil et al. [14]. For the translation of density to elastic modulus, we used the equation:

$$E_{\text{element}} = E_{\text{tissue}} \times (\text{Gray} - \text{value}_{\text{element}})^{\gamma},$$

where the gray-value data was normalised to 900 mg HA/cm^3, γ was set at 1.1, and negative moduli were removed. Analyses were performed blinded to treatment allocation.

Failure load (N) was estimated in the segmented model based on Pistoia's criterion assuming that fracture occurs when 2% of the bone tissue is strained beyond a critical limit of 7,000 μstrain with elastic properties of 10 GPa [13, 27]. However, since the elastic properties in our study were twice as high as those used by Pistoia et al., the critical strain limit in our study was set to 3,500 μstrain in order to calculate comparable failure loads. Stiffness (kN/mm) was assessed with both models. Average values of the von Mises stresses in the trabecular and cortical bone (MPa), which are a measure of the intensity of the internal forces as a reaction to external loading applied on the bone, were computed in the segmented model for a 1,000 N applied load. The polar moment of inertia was calculated as well [28].

Other measurements

Lumbar spine and femoral neck aBMD were measured at baseline, and after 1 and 2 years with dual-energy X-ray absorptiometry (DXA) using Hologic or Lunar devices. Devices were cross-calibrated with an external phantom (European spine phantom; QRM GmbH, Möhrendorf, Germany) to optimize concordance between the centers. Biochemical bone turnover markers were obtained at each visit and were centrally assessed (Supreme, Liège, Belgium). Bone-specific Alkaline Phosphatase (bALP) was assayed by an immunoradiometric assay (Tandem® ROstase®, Beckman Coulter, San Diego, CA, USA) and S-CTX-I by an enzyme-linked immunosorbent assay (Serum CrossLaps® ELISA, Nordic Bioscience Diagnostic, Herlev, Denmark). Adverse events and laboratory parameters were recorded at each visit.

Statistical methods

In this exploratory study, all efficacy analyses were performed in the intention-to-treat (ITT) population (all

randomized patients who had taken at least one dose of study medication and had a baseline and post-baseline assessable by HR-pQCT scan) on non-corrected and non-calibrated data. The safety set was defined as all included patients who took at least one dose of the study treatment. All the analyses described herein were preplanned, and the blinding was not broken for the investigators, the patients, or the sponsor at the time of the interim analysis after 1 year [20].

Baseline characteristics are presented as descriptive statistics. Relative change from baseline to last observation was analyzed using a linear model with center as covariate (fixed effect), and robustness was checked with center as a random effect. A second robustness analysis was performed using a nonparametric approach without adjustment, based on Hodges–Lehmann's estimator. Treatment effect was analyzed using a Student *t*-test or a Wilcoxon signed-ranks test, and treatment groups were compared using Student *t*-test on the overall general linear model (least-squares norm) or a Mann–Whitney–Wilcoxon test when appropriate. Within-group results are presented as means ± SD, or medians when non-normally distributed, and each between-group difference is presented as an estimate (standard error [SE]) with 95% confidence interval (CI). Similar analyses were performed for aBMD and bone turnover markers. Safety data are presented as descriptive statistics. The type I error rate was set at 5%. All statistical analyses were performed on SAS® version 9.1 software.

Results

Figure 1 shows the trial profile. Between January 2006 and February 2007, we randomly allocated 88 patients to strontium ranelate (n=46) or alendronate (n=42) (i.e., the safety set). The ITT population comprised 83 patients (96% of the randomized population; n=42 strontium ranelate; n=41 alendronate). Thirty-one patients left the study; the distribution of withdrawals was well balanced between the groups, and the majority of patients left the study for non-medical reasons. The baseline characteristics of the ITT population are presented in Table 1. There were no relevant differences in demographic, clinical, or HR-pQCT characteristics between the treatment groups. Nearly 25% of the patients had previous osteoporotic peripheral fracture (n=10 strontium ranelate; n=11 alendronate) or vertebral deformities (n=7 strontium ranelate; n=9 alendronate). Mean treatment duration in the safety set was 19.5± 6.8 months (range 1–25 months). The baseline characteristics of the fully completers were identical to those of the ITT population (data not shown). Overall compliance during the 2 years of the study was 90% for sachets and

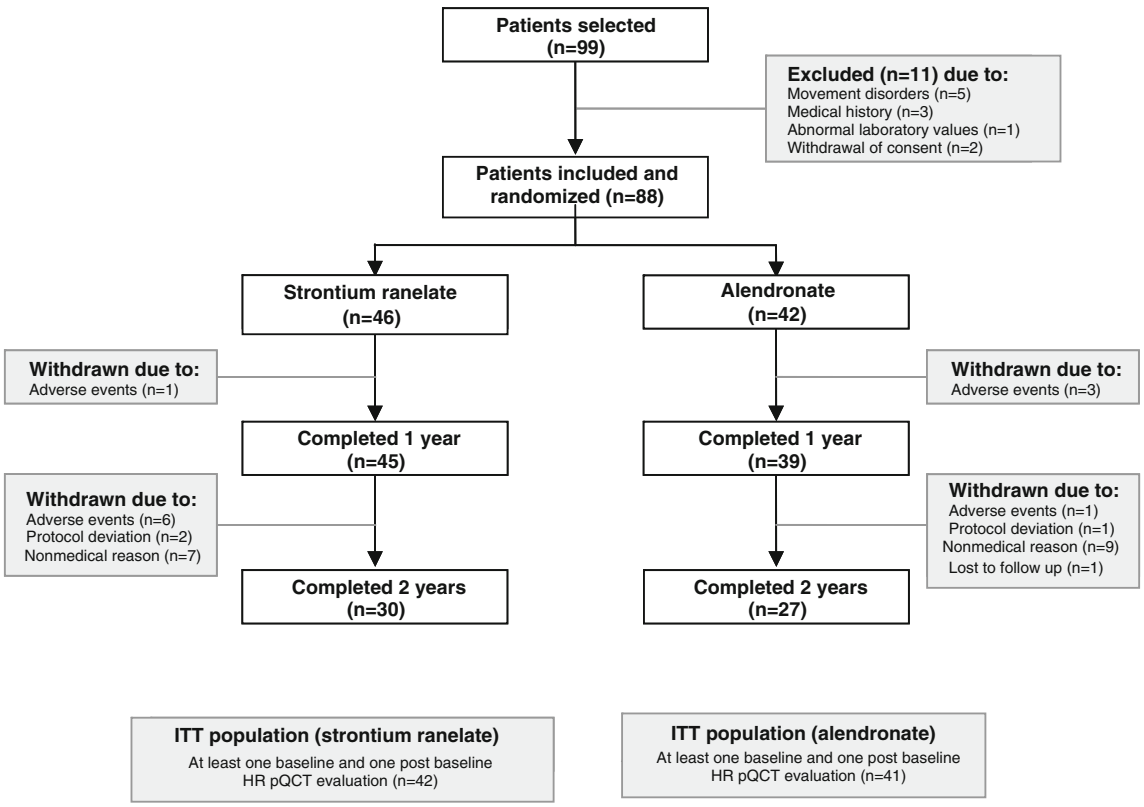

Fig. 1 Trial profile. HR-pQCT, high-resolution peripheral quantitative computed tomography

93% for capsules. The compliance was defined as the number of sachets or capsules taken divided by the theoretical number of sachets or capsules to be taken.

Relative changes in HR-pQCT parameters at last value versus baseline for distal tibia are summarized in Table 2. There were 41 patients with assessable scans at baseline and post-baseline in the strontium ranelate group versus 39 in the alendronate group. Distal tibia cortical parameters CTh and D_{Cort} increased from baseline to last value with strontium ranelate with relative changes of 6.3% and 1.4% ($P<0.0001$ and $P<0.005$, respectively) versus no change with alendronate (0.9% and 0.4%, respectively; both NS). There was a between-group difference for both CTh ($P<0.005$) and D_{Cort} ($P<0.05$). For CTh directly measured using a distance transformation method, the between-group difference of changes from baseline to last value was of lower magnitude, with a P value close to significance ($P=0.060$). The between-group change difference was 2.2±2.2% ($P=0.316$, NS).

For trabecular bone, as assessed with the standard software, the relative change in BV/TV was 2.5% with

Table 1 Baseline characteristics of the intention-to-treat (ITT) population

	Strontium ranelate ($n=42$)	Alendronate ($n=41$)	Whole population ($n=83$)
Demographic characteristics			
Age (years)	63.6±7.5	63.8±7.6	63.7±7.5
Weight (kg)	59.1±9.1	56.5±7.6	57.8±8.5
BMI (kg/m²)	23.1±3.3	22.6±2.7	22.9±3.1
DXA-BMD and T-score			
L1–L4 aBMD (g/cm²)	0.748±0.087	0.735±0.093	0.741±0.089
Lumbar spine T-score	−2.7±0.8	−2.8±0.8	−2.8±0.8
Femoral neck aBMD (g/cm²)	0.619±0.097	0.609±0.094	0.614±0.095
Femoral neck T-score	−2.0±0.8	−2.1±0.8	−2.0±0.8
HR-pQCT parameters (distal tibia)			
D_{Cort} (mg HA/cm^3)	750.3±87.6	745.7±78.1	748.1±82.6
CTh (μm)	721±242	753±263	737±251
Cortical porosity (%)	8.9±3.5	9.2±2.8	9.1±3.1
BV/TV (%)	9.5±2.5	9.3±2.7	9.4±2.6
TbN (mm^{-1})	1.35±0.34	1.25±0.29	1.30±0.32
TbSp (μm)	686±269	713±190	699±233
TbTh (μm)	69±15	73±17	71±16
CSA (mm^2)	835±152	820±161	828±157
Polar moment of inertia (mm^4)	15,481±3,505	13,865±2,909	14,693±3,214
HR-pQCT parameters (distal radius)			
D_{Cort} (mg HA/cm^3)	790.0±92.7	782.9±92.2	786.8±91.9
CTh (μm)	595±176	559±189	579±182
Cortical porosity (%)	4.6±2.2	4.8±1.9	4.7±2.0
BV/TV (%)	8.7±2.7	7.9±2.2	8.3±2.5
TbN (mm^{-1})	1.40±0.31	1.29±0.27	1.35±0.30
TbSp (μm)	651±199	697±192	671±195
TbTh (μm)	60±12	59±11	60±12
CSA (mm^2)	457±84	418±83	440±84
Polar moment of inertia (mm^4)	3,326±735	2,986±744	3,177±739
FEA analysis (segmented model, distal tibia)			
Failure load (N)	6,715±947	6,581±874	6,649±909
Stiffness (kN/mm)	311±49	304±49	307±49
Cortical stress (MPa)	7.13±1.33	7.21±1.06	7.17±1.20
Trabecular stress (MPa)	3.82±0.67	4.03±0.52	3.92±0.61

Values are mean ± SD

BMI body mass index, *aBMD* areal bone mineral density (DXA-BMD), *CSA* cross-sectional area, *BV/TV* bone volume fraction, *CTh* cortical thickness, D_{Cort} cortical bone density, D_{trab} trabecular bone density, *HR-pQCT* high-resolution peripheral quantitative computed tomography, *TbN* trabecular number, *TbSp* trabecular separation, *TbTh* trabecular thickness using standard software

Table 2 High-resolution peripheral quantitative computed tomography HR-pQCT results

	Relative change from baseline for last value (%)		Between-group difference	
	Strontium ranelate (n=42)	Alendronate (n=41)	E (SE), 95% CI	P value[†]
Distal tibia				
Patients with assessable scans at baseline and post-baseline	41	39		
D_{Cort}	1.4±2.8**	0.4±2.1	1.1 (0.5), 0.1 to 2.2	<0.05
CTh	6.3±9.5****	0.9±6.2	5.4 (1.8), 1.8 to 9.1	<0.05
	[2.1±3.1]	[0.6±4.2]	[1.6 (0.8), −0.7 to 3.2]	0.06
BV/TV	2.5±5.1****	0.8±3.8	1.8 (0.9), 0.1 to 3.5	<0.05
TbN	3.6±9.3*	4.6±10.0*	−1.1 (2.1), −5.2 to 3.1	0.61
	[3.5±9.2]	[4.6±10.0]	[−1.1 (2.1), −5.3 to 2.9]	0.58
TbSp	−3.0±8.7*	−3.6±9.7*	0.7 (2.0), −3.2 to 4.7	0.72
	[−2.5±8.5]	[−3.2±9.5]	[0.8 (2.0), −3.1 to 4.7]	0.70
TbTh	−0.5±8.7	−3.0±8.1*	2.6 (1.9), −1.2 to 6.4	0.18
	[+0.3±2.0]	[−0.4±1.7]	[0.7 (0.4), −0.1 to 1.5]	0.09
Cortical porosity	3.8±12.1	1.4±7.0	2.2 (2.2), −2.1 to 6.6	0.31
Polar moment of inertia	1.8±3.3	0.5±3.9	1.4 (0.8), −0.2 to 3.0	0.09
Distal radius				
Patients with assessable scans at baseline and post-baseline	36	28		
D_{Cort}	1.1±2.5	−0.3±1.9	1.2 (0.5), 0.1 to 2.2	<0.05
CTh	0.8±6.6	−1.0±7.2	1.2(1.6), −2.0 to 4.3	0.46
BV/TV	0.0±4.1	−1.4±4.7	1.7 (1.0), −0.2 to 3.6	0.07
TbN	0.3±5.7	−1.3±4.9	1.3 (1.6), −1.4 to 4.1	0.33
TbSp	0.01±6.2	1.6±5.2	−1.3 (1.5), −4.2 to 1.7	0.39
TbTh	−0.1±6.0	−0.2±6.3	0.8 (1.3), −1.9 to 3.5	0.56
Cortical porosity	0.1±12.0	0.7±9.5	−0.5 (2.9), −6.3 to 5.2	0.85
Polar moment of inertia	−0.4±2.9	−0.3±3.1	−0.4 (0.7), −1.7 to 1.0	0.61

Values are means ± SD. The values were obtained with the standard software. In brackets are the results obtained with the direct transformation software

E (SE) estimate of the adjusted mean difference (standard error), *CI* confidence interval of estimate

[†] P value for between group difference strontium ranelate versus alendronate (parametric approach)

*P<0.05, **P<0.005, ***P<0.0005, ****P<0.0001 last value versus baseline (two-sided Student'st-test for paired samples)

strontium ranelate from baseline to last value (P<0.0001) versus 0.8% with alendronate (NS), with a significant between-group difference (P<0.05). TbN significantly increased by last value in both groups with a relative change of 3.6% with strontium ranelate and 4.6% with alendronate (both P<0.05 versus baseline). TbSp decreased with a relative change of −3.0% with strontium ranelate and −3.6% with alendronate (both P<0.05 versus baseline), while TbTh remained unchanged with strontium ranelate (−0.5%, NS) and decreased with alendronate (−3.0%, P< 0.05). TbN, TbSp, and TbTh analysis by distance transformation provided qualitatively similar results to those obtained with the standard software.

Figure 2 presents the progression of distal tibia CTh and BV/TV throughout the study. Progressive increases were recorded in both parameters with strontium ranelate from the third month onward. The changes of CTh and BV/TV from baseline with strontium ranelate were significant from the third month onward for CTh and from the sixth month onward for BV/TV. The change from baseline with strontium ranelate was significantly different from that with alendronate after 3 months, 1 year, and 2 years.

The number of assessable scans for the distal radius was lower (36 in the strontium ranelate group and 28 in the alendronate group) than for the distal tibia. This was mainly due to a higher number of scans with movement artifacts. The changes in HR-pQCT parameters for the distal radius were smaller (Table 2). At last value, distal radius D_{Cort} increased with a relative change of 1.1% with strontium ranelate (P< 0.05 versus baseline), but not with alendronate (−0.3%, NS),

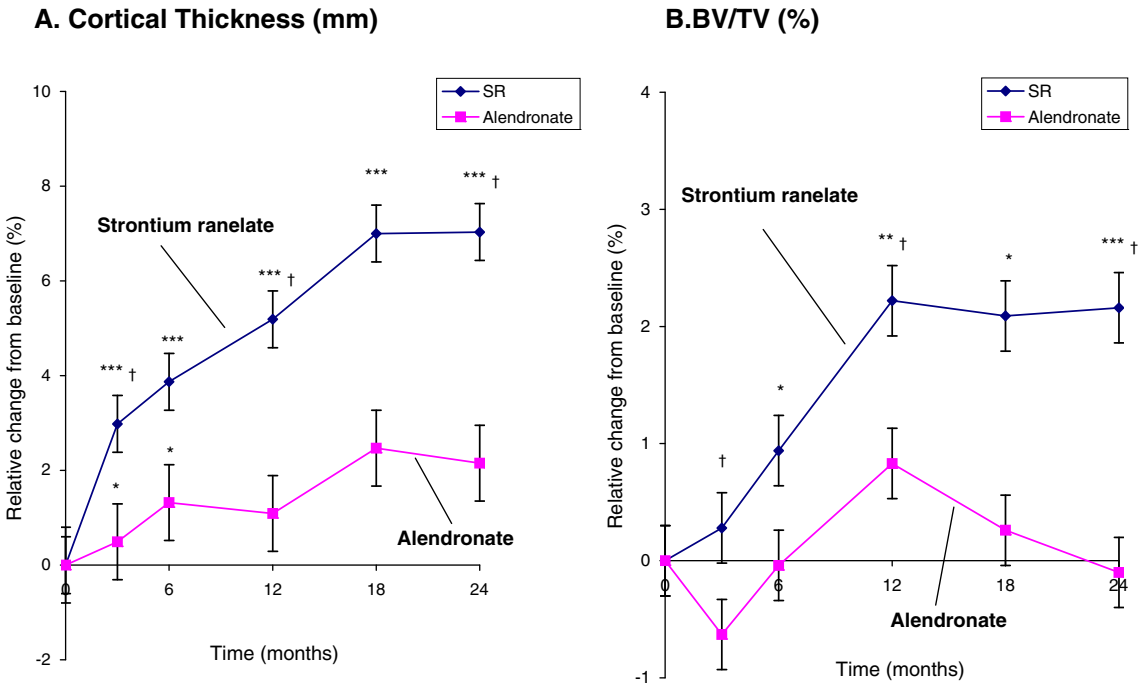

Fig. 2 Change in cortical thickness (**A**) and bone volume fraction (BV/TV) (**B**) in distal tibia throughout the duration of the study (relative change from baseline ± SD). *P<0.05; **P<0.01; ***P<0.001 versus baseline. †P<0.05 strontium ranelate versus alendronate

with a significant between-group difference (E [SE], 1.2 [0.5], 95% CI, 0.1–2.2, P<0.05). There were no other statistically different relative changes in the other parameters for distal radius over time or between the groups.

FEA results in the ITT population (41 patients for strontium ranelate and 39 for alendronate) are presented in Fig. 3 for failure load, and for trabecular and cortical stresses in the segmented model. Failure load increased with strontium ranelate with a relative change of 2.1% at last value (P<0.005 versus baseline) versus no change with alendronate (−0.6%, NS). This led to a significant between-group difference in failure load (P<0.01). Treatment with strontium ranelate was associated with lower trabecular and cortical stresses, with relative changes of −2.4% (P<0.005 versus baseline) and −1.6% (P<0.05 versus baseline), respectively. Trabecular stress decreased with alendronate (relative change, −2.0%, P<0.01 versus baseline), but cortical stress did not (relative change 1.0%, NS). There was therefore a significant between-group difference for cortical stress (P<0.05), but not for trabecular stress. Depending on the segmented or gray-level μFEA model applied, stiffness was either maintained (relative change 1.2%, P=0.074) or increased (3.1%, P<0.001) with strontium ranelate, and decreased (−1.7%, P<0.05) or maintained (0.7%, NS) with alendronate. For both models, a between-group difference was observed for stiffness (P<0.05 for both). The difference in polar moment of inertia between last measurement and baseline was 1.8±3.3% and 0.5±3.9% for strontium ranelate and alendronate, respectively, with a between-group difference of 1.4±0.8% (P=0.095).

Mean lumbar spine aBMD increased in all patients, by 6.5±6.3% with strontium ranelate and 5.6±4.3% with alendronate. Femoral neck BMD increased as well (4.7±4.3% and 3.3±4.0%, respectively). The increase in lumbar spine and femoral neck BMD over time was statistically significant in both groups (all P<0.0001), without any between-group difference.

The changes in bone turnover markers are presented in Fig. 4. Both agents reduced S-CTX-I from the third month of treatment, with larger reductions for alendronate. The S-CTX-I values were significantly different from baseline by 3 and 6 months (P<0.05), 18 and 24 (both P<0.005) with strontium ranelate and at all time-points with alendronate (all P<0.0001). By 2 years, the median change from baseline was −16% and −59% for strontium ranelate and alendronate, respectively. In contrast, b-ALP increased from the third month with strontium ranelate, with significant changes by months 3, 18 (P<0.005) and 24 (median change +18%, P<0.0005). At all time points the decrease in b-ALP was significant with alendronate (all P<0.0001), with a median change from baseline to last value of −31%. The between-group difference was significant for both markers at all time points (all P<0.001).

The rate of treatment-related emergent adverse events was similar in both groups (16 with strontium ranelate and

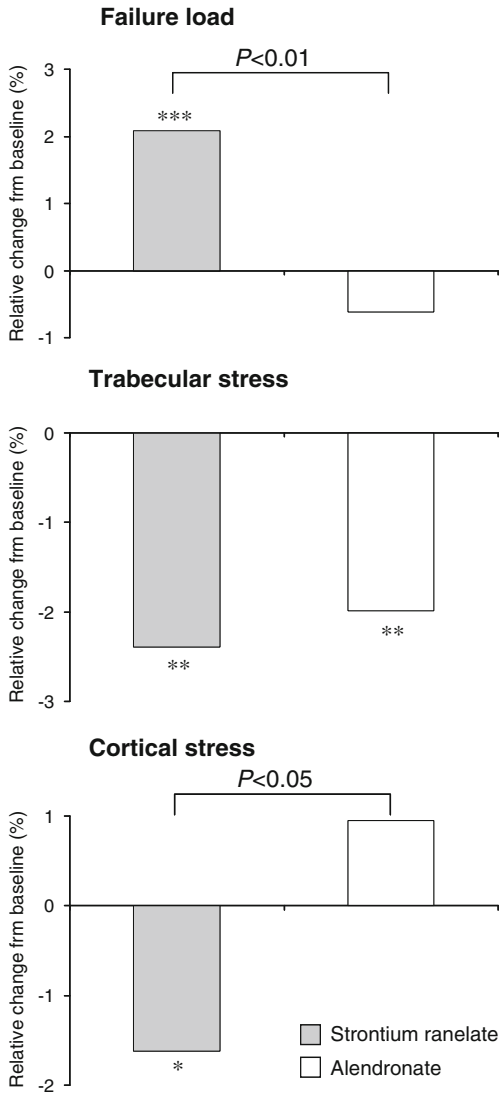

Fig. 3 Finite element analysis results in the segmented model for failure load and trabecular and cortical stress (relative change from baseline ± SD). *P<0.05; **P<0.01; ***P<0.005 versus baseline. P values between groups are for multiple comparisons (Bonferroni criterion)

14 with alendronate), and these events were most frequently related to gastrointestinal disorders (7 and 10, respectively). Adverse events leading to premature treatment withdrawal occurred in 11 patients (seven with strontium ranelate and four with alendronate). Two of these events in the strontium ranelate group were related to cutaneous disorders (pruritic rash and rash, both of mild intensity) and one event to a vascular disorder (superficial phlebitis of mild intensity). Three of the events in the alendronate group were related to gastrointestinal disorders (nausea, upper abdominal pain, and peptic ulcer, of moderate intensity for all three). There were no clinically relevant changes over time or between-group difference in laboratory values or vital signs.

Discussion

This HR-pQCT study indicates that treatment with strontium ranelate is associated with changes in distal tibia cortical and trabecular structure and density, i.e., significant increases in cortical thickness, cortical and trabecular bone density. These changes were already detected by 3 months of treatment and continued up to 2 years. Alendronate maintained these bone parameters at their initial level. Trabecular number increased with both treatments (without any difference between groups), whereas trabecular separation decreased. There was no change in trabecular thickness with strontium ranelate but a decrease with alendronate.

Our 2-year results extend and consolidate the 1-year results in the same population [20], and demonstrate that the differences between the two treatments continue to increase beyond 1 year. Our analysis also indicates that the changes in bone microstructure with strontium ranelate parallel higher failure load, lower cortical and trabecular stresses, an increase in lumbar and femoral neck DXA-determined aBMD together with a modest increase in the bone-formation marker bone specific alkaline phosphatase and a decrease in the bone resorption marker CTX.

A possible influence of edge detection artifacts on our findings was extensively discussed in the report of the 1-year results of this trial [20]. Such an influence could potentially affect both HR-pQCT and FEA parameters, and could be a concern in both arms of our study. Indeed, both strontium having an atomic number of twice that of calcium, and alendronate associated with a higher mean degree of mineralization could influence x-ray attenuation [29]. However, bone strontium content is low after 2 years of treatment (about 1%). Based on bone strontium content estimation and theoretical calculations, such an amount may contribute to an overestimation of cortical thickness by around 2% [30]. On the other hand, there was no correlation between distal tibia cortical thickness and serum strontium levels (R^2=0.17, P=0.292). By the third month of treatment, when some structural changes were already detected, bone strontium content was considerably lower than 1%, reducing thereby the likelihood that the changes observed were entirely due to strontium in bone [20]. By 3 months, cortical density between-group difference was 0.5 (0.3) [0.0; 1.1], P=0.04, and 0.2 (0.3) [−0.4; 0.7], P= 0.6 (mean SE) [95% CI] at distal tibia and distal radius, respectively. Furthermore, when HR-pQCT values were obtained using a distance transformation method, hence with parameters less influenced by density, difference between both groups was of lower magnitude, but close to significance (P=0.060). However, an increase in cortical thickness could result from an increase in cortical area as the result from a reduction in cortical porosity. Indeed, the cortical compartment comprises mineralized matrix and

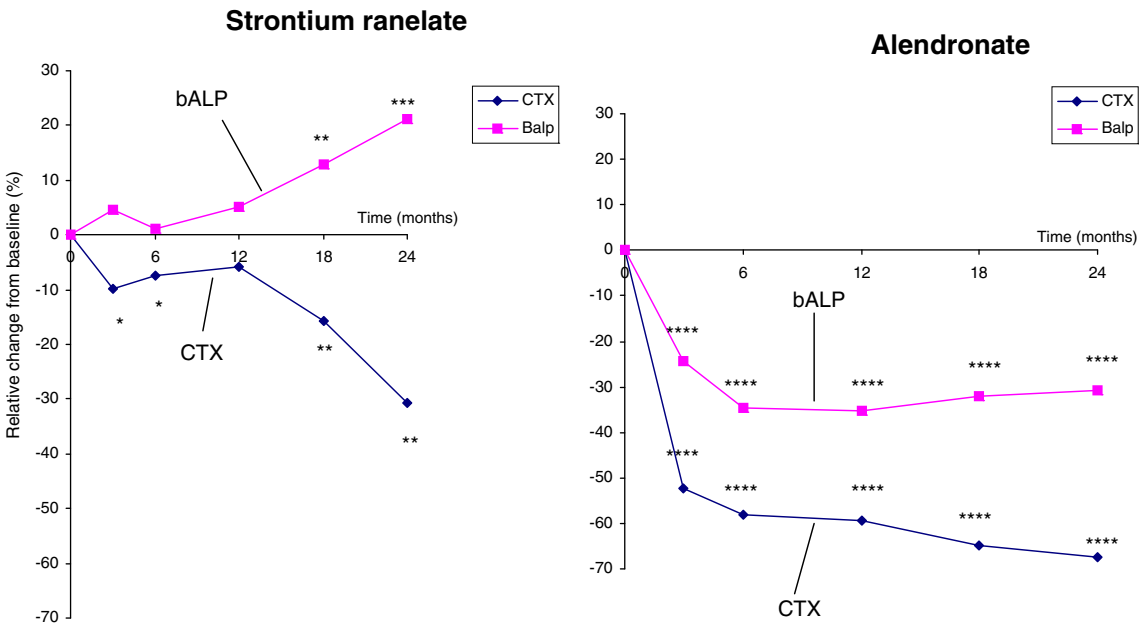

Fig. 4 Median changes in bone markers: bone alkaline phosphatase (b-ALP) for bone formation and C-telopeptide crosslinks of type-1 collagen (S-CTX) for bone resorption in the intention-to-treat (ITT) population. *P<0.05; **P<0.005; ***P<0.0005; ****P<0.0001 versus baseline

pores. If porosity is reduced, as for instance by filling the holes with mineralized bone, the cortical compartment will thus increase [31]. However, the evaluation of cortical porosity did not support this hypothesis.

Our results are in agreement with previous μCT analyses of 41 biopsies from SOTI and TROPOS trials, which reported increased cortical thickness (P=0.008) and decreased trabecular separation (P=0.041) with strontium ranelate versus placebo over 3 years, but no significant change in BV/TV [17]. Another biopsy study performed in ten patients previously treated with bisphophonates, who had paired biopsies before and after 1 year of strontium ranelate treatment, has demonstrated a significant increase in relative bone volume, as assessed by histomorphometry, a technique which is not influenced by the presence of strontium in bone [32].

The results for alendronate in this study contrast with recent HR-pQCT results, which indicate an increase in cortical thickness versus placebo with alendronate, and no change in trabecular number, thickness, and separation [33, 34]. Recent studies have reported increased BMD with bisphosphonate treatment, as measured by QCT or HR-pQCT (at the radius and tibia for alendronate; and at total hip for ibandronate) [31, 33, 34]. Regarding the groups treated with alendronate, the patients in our study were older, had slightly lower lumbar spine aBMD, and received less vitamin D. These discrepancies highlight the need for further HR-pQCT analyses or biopsy studies with bisphosphonates. Regarding bone anabolic agents, the only published report to date failed to find clear HR-pQCT changes in bone structure in patients receiving teriparatide [35], while other histomorphometric and μCT evidences have demonstrated anabolic effects of teriparatide [36–38]. This was attributed in part to the fact that the majority of the study population had previously received bisphosphonate therapy (ten out of 11 patients), which may have blunted the bone response to an anabolic agent [35].

We used FEA based on binary and gray-level HR-pQCT images to estimate failure load, cortical and trabecular stresses, and stiffness of treated bone. As emphasized by Burghardt et al. [33], the use of FEA based on binary HR-pQCT data helps to understand how microstructural changes in response to treatment affect biomechanical parameters, but fails to indicate changes in mineral composition, which, supposedly, are a significant factor in the anti-fracture efficacy of anti-resorptive therapies. However, one limitation of the gray-level model is that the exact relationship between the element gray-value and the element elastic modulus is presently not available for the tibia. Therefore, we do not have any information in human on the influence of strontium on this analysis. Our results indicate that treatment with strontium ranelate is associated with greater failure load and lower cortical stress than alendronate. Both treatments improved trabecular stress. Depending on the model applied, stiffness was either maintained or increased with strontium ranelate, and maintained or decreased with alendronate. These results

also compare well with those reported for ibandronate, which increased trabecular parameters but not cortical parameters [31], as well as with those reported for alendronate showing no significant difference in tibial stiffness and failure load after 2 years of treatment [33]. The impact of strontium ranelate on cortical bone is of particular interest, since recent findings suggest that cortical bone may be a more important target for the treatment of osteoporosis than previously thought [39, 40]. Both agents reduce fracture risk, whereas only strontium ranelate improves FEA parameters. We could, therefore, hypothesize that alendronate's anti-fracture efficacy may be related to a modification of bone metabolism and a change in the intrinsic matrial properties of bone in terms of mineralization and aBMD [29]. In an experimental study, FEA was applied to the vertebral body of rats treated with strontium ranelate for 2 years [41]. FE simulations showed a 29% higher strength and a 22% higher stiffness with strontium treatment, which were related to greater cortical and trabecular thickness, together with a 7% decrease in tissue level stresses. Thus, these experimental data are in agreement with those of the present study in human. On the other hand, while strontium ranelate's anti-fracture efficacy is linked to an increase in aBMD [42], the improvement in structure would contribute to a higher resistance to fracture. The increases in lumbar spine and femoral neck BMD are in line with the results of phase 3 studies with both agents [15, 16, 18].

The possibility of edge detection artifacts as described above and the sample size limit our study. Another limitation is the lack of clear differences at the distal radius, due to difficulties in measurement (28% of radius images were not readable, mainly due to movement artifacts) and the small effect sizes at this site. The absence of effect may also be related to the fact that radius is not a weight-bearing bone, with possibly different bone turnover responses. In this context, we should note that the change in aBMD at the radius level is usually smaller than at other sites, regardless of the anti-osteoporotic treatment. This appears to complicate detection of changes in structure at this site. The distal tibia, however, has been shown to be a relevant site since distal tibia HR-pQCT values are associated with fractures to the same extent as at the radius [43]. This selective difference in structural responses between distal radius and tibia is puzzling, and could even support that the changes observed at the tibia level cannot solely be attributed to strontium-mediated edge detection modification. Indeed, at both skeletal sites, the increase with strontium ranelate in cortical volumetric density was identical, implying that the structural variables should be similarly influenced. However, this is not the case, since there was an increase in CTh at tibia, but not at radius levels.

Within the constraints of the method, and while a possible artefactual contribution of strontium cannot be quantified, altogether our results are compatible with strontium ranelate-mediated changes in distal tibia bone structure as assessed with HR-pQCT and FEA-determined biomechanically relevant parameters, greater than with alendronate. However, the magnitude of the differences is unclear and requires confirmation with another method.

Acknowledgements The study was sponsored by Servier.

Conflicts of interest All authors are investigators in the study, except A. Laib, who was responsible for central reading of HR-pQCT parameters, and S. Boutroy, who was responsible for central reading of FEA parameters.

References

1. Bouxsein ML, Seeman E (2009) Quantifying the material and structural determinants of bone strength. Best Pract Res Clin Rheumatol 23(6):741–753
2. Seeman E, Delmas PD (2006) Bone quality–the material and structural basis of bone strength and fragility. N Engl J Med 354 (21):2250–2261
3. Griffith JF, Genant HK (2008) Bone mass and architecture determination: state of the art. Best Pract Res Clin Endocrinol Metab 22(5):737–764
4. Adams JE (2009) Quantitative computed tomography. Eur J Radiol 71(3):415–424
5. Laib A, Ruegsegger P (1999) Calibration of trabecular bone structure measurements of in vivo three-dimensional peripheral quantitative computed tomography with 28-micron-resolution microcomputed tomography. Bone 24(1):35–39
6. MacNeil JA, Boyd SK (2007) Accuracy of high-resolution peripheral quantitative computed tomography for measurement of bone quality. Med Eng Phys 29(10):1096–1105
7. Vico L, Zouch M, Amirouche A, Frere D, Laroche N, Koller B et al (2007) High-resolution pQCT analysis at the distal radius and tibia discriminates patients with recent wrist and femoral neck fractures. J Bone Miner Res 23(11):1741–1750
8. Sornay-Rendu E, Boutroy S, Munoz F, Delmas PD (2007) Alterations of cortical and trabecular architecture are associated with fractures in postmenopausal women, partially independent of decreased BMD measured by DXA: the OFELY study. J Bone Miner Res 22(3):425–433
9. Sornay-Rendu E, Cabrera-Bravo JL, Boutroy S, Munoz F, Delmas PD (2009) Severity of vertebral fractures is associated with alterations of cortical architecture in postmenopausal women. J Bone Miner Res 24(4):737–743
10. Sornay-Rendu E, Boutroy S, Munoz F, Bouxsein ML (2009) Cortical and trabecular architecture are altered in postmenopausal women with fractures. Osteoporos Int 20(8):1291–1297
11. Boutroy S, Bouxsein ML, Munoz F, Delmas PD (2005) In vivo assessment of trabecular bone microarchitecture by high-resolution peripheral quantitative computed tomography. J Clin Endocrinol Metab 90(12):6508–6515
12. MacNeil JA, Boyd SK (2007) Load distribution and the predictive power of morphological indices in the distal radius and tibia by high resolution peripheral quantitative computed tomography. Bone 41(1):129–137

13. Pistoia W, Van Rietbergen B, Lochmuller EM, Lill CA, Eckstein F, Ruegsegger P (2002) Estimation of distal radius failure load with micro-finite element analysis models based on three-dimensional peripheral quantitative computed tomography images. Bone 30 (6):842–848
14. MacNeil JA, Boyd SK (2008) Bone strength at the distal radius can be estimated from high-resolution peripheral quantitative computed tomography and the finite element method. Bone 42 (6):1203–1213
15. Meunier PJ, Roux C, Seeman E, Ortolani S, Badurski JE, Spector TD et al (2004) The effects of strontium ranelate on the risk of vertebral fracture in women with postmenopausal osteoporosis. N Engl J Med 350(5):459–468
16. Reginster JY, Seeman E, De Vernejoul MC, Adami S, Compston J, Phenekos C et al (2005) Strontium ranelate reduces the risk of nonvertebral fractures in postmenopausal women with osteoporosis: Treatment of Peripheral Osteoporosis (TROPOS) study. J Clin Endocrinol Metab 90(5):2816–2822
17. Arlot ME, Jiang Y, Genant HK, Zhao J, Burt-Pichat B, Roux JP et al (2008) Histomorphometric and microCT analysis of bone biopsies from postmenopausal osteoporotic women treated with strontium ranelate. J Bone Miner Res 23(2):215–222
18. Black DM, Cummings SR, Karpf DB, Cauley JA, Thompson DE, Nevitt MC et al (1996) Randomised trial of effect of alendronate on risk of fracture in women with existing vertebral fractures. Fracture Intervention Trial Research Group. Lancet 348(9041):1535–1541
19. Chavassieux PM, Arlot ME, Reda C, Wei L, Yates AJ, Meunier PJ (1997) Histomorphometric assessment of the long-term effects of alendronate on bone quality and remodeling in patients with osteoporosis. J Clin Invest 100(6):1475–1480
20. Rizzoli R, Laroche M, Krieg MA, Frieling I, Thomas T, Delmas P et al (2010) Strontium ranelate and alendronate have differing effects on distal tibia bone microstructure in women with osteoporosis. Rheumatol Int 30(10):1341–1348
21. Laib A, Hildebrand T, Hauselmann HJ, Ruegsegger P (1997) Ridge number density: a new parameter for in vivo bone structure analysis. Bone 21(6):541–546
22. Parfitt AM, Mathews CH, Villanueva AR, Kleerekoper M, Frame B, Rao DS (1983) Relationships between surface, volume, and thickness of iliac trabecular bone in aging and in osteoporosis. Implications for the microanatomic and cellular mechanisms of bone loss. J Clin Invest 72(4):1396–1409
23. Burghardt AJ, Kazakia GJ, Ramachandran S, Link TM, Majumdar S (2010) Age- and gender-related differences in the geometric properties and biomechanical significance of intracortical porosity in the distal radius and tibia. J Bone Miner Res 25(5):983–993
24. Nishiyama KK, Macdonald HM, Buie HR, Hanley DA, Boyd SK (2010) Postmenopausal women with osteopenia have higher cortical porosity and thinner cortices at the distal radius and tibia than women with normal aBMD: an in vivo HR-pQCT study. J Bone Miner Res 25(4):882–890
25. Van Rietbergen B, Weinans H, Huiskes R, Odgaard A (1995) A new method to determine trabecular bone elastic properties and loading using micromechanical finite-element models. J Biomech 28(1):69–81
26. Homminga J, Huiskes R, Van Rietbergen B, Ruegsegger P, Weinans H (2001) Introduction and evaluation of a gray-value voxel conversion technique. J Biomech 34(4):513–517
27. Turner CH, Rho J, Takano Y, Tsui TY, Pharr GM (1999) The elastic properties of trabecular and cortical bone tissues are similar: results from two microscopic measurement techniques. J Biomech 32(4):437–441
28. Turner CH, Burr DB (1993) Basic biomechanical measurements of bone: a tutorial. Bone 14(4):595–608
29. Boivin GY, Chavassieux PM, Santora AC, Yates J, Meunier PJ (2000) Alendronate increases bone strength by increasing the mean degree of mineralization of bone tissue in osteoporotic women. Bone 27(5):687–694
30. Boivin G, Farlay D, Khebbab MT, Jaurand X, Delmas PD, Meunier PJ. (2010) In osteoporotic women treated with strontium ranelate, strontium is located in bone formed during treatment with a maintained degree of mineralization. Osteoporos Int 21 (4):667–677
31. Lewiecki EM, Keaveny TM, Kopperdahl DL, Genant HK, Engelke K, Fuerst T et al (2009) Once-monthly oral ibandronate improves biomechanical determinants of bone strength in women with postmenopausal osteoporosis. J Clin Endocrinol Metab 94 (1):171–180
32. Busse B, Jobke B, Hahn M, Priemel M, Niecke M, Seitz S et al (2010) Effects of strontium ranelate administration on bisphosphonate-altered hydroxyapatite: matrix incorporation of strontium is accompanied by changes in mineralization and microstructure. Acta Biomater 6(12):4513–4521
33. Burghardt AJ, Kazakia GJ, Sode M, de Papp AE, Link TM, Majumdar S (2010) A longitudinal HR-pQCT study of alendronate treatment in postmenopausal women with low bone density: relations among density, cortical and trabecular microarchitecture, biomechanics, and bone turnover. J Bone Miner Res 25(12):2558–2571
34. Seeman E, Delmas PD, Hanley DA, Sellmeyer D, Cheung AM, Shane E et al (2010) Microarchitectural deterioration of cortical and trabecular bone: differing effects of denosumab and alendronate. J Bone Miner Res 25(8):1886–1894
35. Macdonald HM, Nishiyama KK, Hanley DA, Boyd SK (2011) Changes in trabecular and cortical bone microarchitecture at peripheral sites associated with 18 months of teriparatide therapy in postmenopausal women with osteoporosis. Osteoporos Int 22 (1):357–362
36. Dempster DW, Cosman F, Kurland ES, Zhou H, Nieves J, Woelfert L et al (2001) Effects of daily treatment with parathyroid hormone on bone microarchitecture and turnover in patients with osteoporosis: a paired biopsy study. J Bone Miner Res 16(10):1846–1853
37. Hodsman AB, Kisiel M, Adachi JD, Fraher LJ, Watson PH (2000) Histomorphometric evidence for increased bone turnover without change in cortical thickness or porosity after 2 years of cyclical hPTH(1–34) therapy in women with severe osteoporosis. Bone 27 (2):311–318
38. Jiang Y, Zhao JJ, Mitlak BH, Wang O, Genant HK, Eriksen EF (2003) Recombinant human parathyroid hormone (1–34) [teriparatide] improves both cortical and cancellous bone structure. J Bone Miner Res 18(11):1932–1941
39. Zebaze RM, Ghasem-Zadeh A, Bohte A, Iuliano-Burns S, Mirams M, Price RI et al (2010) Intracortical remodelling and porosity in the distal radius and post-mortem femurs of women: a cross-sectional study. Lancet 375(9727):1729–1736
40. Burr DB (2010) Cortical bone: a target for fracture prevention? Lancet 375(9727):1672–1673
41. Boyd SK, Szabo E, Ammann P (2011) Increased bone strength is associated with improved bone microarchitecture in intact female rats treated with strontium ranelate: a finite element analysis study. Bone 48(5):1109–1116
42. Bruyere O, Roux C, Detilleux J, Slosman DO, Spector TD, Fardellone P et al (2007) Relationship between bone mineral density changes and fracture risk reduction in patients treated with strontium ranelate. J Clin Endocrinol Metab 92(8):3076–3081
43. Vilayphiou N, Boutroy S, Sornay-Rendu E, Van Rietbergen B, Munoz F, Delmas PD et al (2010) Finite element analysis performed on radius and tibia HR-pQCT images and fragility fractures at all sites in postmenopausal women. Bone 46(4):1030–1037